Casimir force between hyperbolic metamaterials

Ge Song,[1,2,3] Jingping Xu,[1,4,*] Chengjie Zhu,[1] Pengfei He,[3] Yaping Yang,[1,†] and Shi-Yao Zhu[4,5,6]

[1]*MOE Key Laboratory of Advanced Micro-Structured Materials, School of Physics Science and Engineering, Tongji University, Shanghai 200092, China*

[2]*College of Information Technology, Shanghai Ocean University, Shanghai 201306, China*

[3]*School of Aerospace Engineering and Applied Mechanics, Tongji University, Shanghai 200092, China*

[4]*Beijing Computational Science Research Center, Beijing 100084, China*

[5]*Department of Physics, Zhejiang University, Hangzhou 310027, China*

[6]*Synergetic Innovation Center of Quantum Information and Quantum Physics, University of Science and Technology of China, Hefei, Anhui 230026, China*

(Received 13 September 2016; published 7 February 2017)

The Casimir force between two hyperbolic metamaterials (HMMs) constructed by alternative metal-dielectric layers is investigated. Due to the existence of the hyperbolic dispersion, the electromagnetic response of HMMs becomes extremely dramatic, which is embodied by the nearly total reflection in such frequency region. As a result, the Casimir force between HMMs is much greater than that between ordinary dielectrics. In addition, it is shown that the Casimir force is proportional to the bandwidth of this hyperbolic dispersion, which is dependent on the filling factor as well as the characteristic frequencies of ingredient materials. Therefore, the relations between the force and these parameters are discussed. We show that the Casimir force can be controlled by tuning the bandwidth possessing hyperbolic dispersion of the structures. This work provides promising applications of HMMs on microelectromechanical systems and nanoelectromechanical systems.

DOI: 10.1103/PhysRevA.95.023814

I. INTRODUCTION

The Casimir effect, which exists between neutral bodies, is a macroscopic quantum effect that results from the change of the electromagnetic vacuum zero-point energy due to the existence of the boundaries. In 1948, Casimir [1] theoretically predicted the attractive interaction between two parallel, neutral perfectly conducting plates in vacuum. In 1956, Lifshitz [2] generalized Casimir's theory to consider the force between a pair of semi-infinite dielectric slabs containing dispersion and absorption in finite temperature. With the advances in microelectromechanical and nanoelectromechanical systems (MEMS and NEMS), progress has been made in the theoretical understanding and experimental measurements of the Casimir effect among various materials with different geometries [3–8]. As the attractive force could lead to the irreversible adhesion of the neighboring elements, the switch of the Casimir force from attractive to repulsive has attracted extensive attention [9–11] and was found to be related to the symmetry of electric and magnetic properties of two plates [9]. Therefore, how to control the Casimir effect by special materials with controllable electromagnetic properties becomes a hot point [12,13]. For instance, the Casimir effect between two metamaterials [14–16], saturated ferrite materials [17], or composite materials [18–22] has been discussed. In addition, graphene [23] and the quantum state of matter named topological insulator [24–26] have also been used to control the Casimir effect.

Recently, a new kind of man-made metamaterial named hyperbolic metamaterials (HMMs) has attracted a great deal of attention [27]. Such artificial medium is extremely anisotropic and one of the diagonal elements of its effective permittivity tensor is negative in a broad frequency region [28], which leads to the hyperbolic isofrequency contour. Therefore people name this class of artificial media as hyperbolic metamaterials (HMMs). Furthermore, we use the hyperbolic dispersion region to indicate a frequency region possessing hyperbolic isofrequency contour of HMMs. Due to the hyperbolic dispersion, HMMs provide novel electromagnetic modes with high wave vectors [29]. Its promising applications have been reported, including negative refraction [30], efficient single-photon sources [31–33], heat transport [34,35], and subdiffraction imaging [36,37]. Generally, HMMs across the optical spectrum have been realized by alternative metal-dielectric layered structures [30,32,36] or metallic nanowire arrays embedded in a dielectric host [38,39]. Here we focus on the HMMs made of layered metal-dielectric structures since such kind of HMMs is easy to be fabricated in experiment and can be theoretically described by the effective medium theory.

Actually, HMMs are also a special kind of composite medium. In previous works, the Casimir effect between composite materials made of a homogeneous matrix with spherical or elliptical metallic particles is presented [19–22]. In these works the composite materials are treated as isotropic materials by different effective medium approximations. The choice of effective medium approximation depends on the filling factor and the particles' shape [40], and in turn determinates the feature of the Casimir force involved [20]. As HMMs are anisotropic composite materials made of alternatively metal and dielectric layers, they cannot be treated as an isotropic effective medium and can be only correctly described by the anisotropic Maxwell Garnett mixing formula [40], which is quite different from previous works [19–22]. Therefore, the influence of the anisotropic as well as the hyperbolic dispersion of HMMs on the Casimir force is interesting and is the topic of this paper.

The paper is arranged as follows: In Sec. II, we introduce the model and theoretical framework including the Casimir force between two slabs and the characters of HMMs. In

*xx_jj_pp@hotmail.com

†yang_yaping@tongji.edu.cn

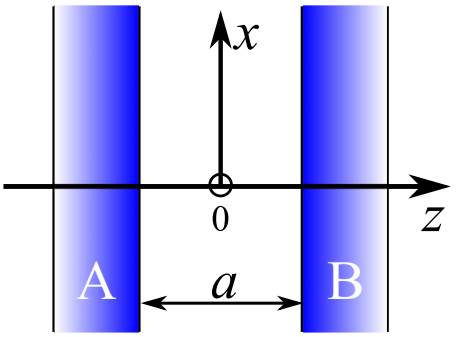

FIG. 1. Scheme of the system considered.

Sec. III, we perform the calculation of the Casimir force between two HMMs. To highlight the advantage of HMMs compared with the normal dielectric slab, the influence of the adjustable parameters of HMMs on the Casimir force are analyzed in detail. These parameters include the filling factor and characteristic frequencies of ingredient materials, i.e., dielectric and metal. In Sec. IV, we draw the conclusion.

II. MODEL AND THEORETICAL FRAMEWORK

The scheme of the system considered here is depicted in Fig. 1. Two parallel HMM slabs, i.e., A and B, are separated by a distance a in free space. The x-y plane is set to be parallel to the surfaces of the slabs, while the z axis is perpendicular to the surfaces and is the out-of-plane optical axis of the uniaxial anisotropic HMM slabs.

A. Casimir force between parallel slabs

Based on the Maxwell electromagnetic stress tensor method with the macroscopic field operators, the Casimir force at zero temperature can be expressed as

$$F_{\mathrm{C}} = -\frac{\hbar}{\pi}\mathrm{Re}\int_0^\infty d\omega \iint \frac{d^2\mathbf{k}}{(2\pi)^2}\sqrt{\frac{\omega^2}{c^2}-k^2} \times \sum_{p=\mathrm{TE,TM}} \frac{r_p^{\mathrm{A}}(\omega,k)r_p^{\mathrm{B}}(\omega,k)e^{2ia\sqrt{\omega^2/c^2-k^2}}}{1-r_p^{\mathrm{A}}(\omega,k)r_p^{\mathrm{B}}(\omega,k)e^{2ia\sqrt{\omega^2/c^2-k^2}}}, \quad (1)$$

where the integral is carried out over all electromagnetic modes marked by frequency ω and the component of wave vector parallel to surface $\mathbf{k}$. $r_p^{\mathrm{A(B)}}$ is the reflection coefficient of the slab A (B) for the p polarized wave. Here we stress that Eq. (1) is only suitable for cases in which two polarizations (TE and TM) are principal and do not get mixed at any incident angle. The reflection on isotropic media or uniaxial (out-of-plane) planar media without an off-diagonal index tensor meets such requirement. Otherwise the reflection coefficients will be replaced by reflection matrices [14]. In order to avoid all the singularities, it is convenient to convert the integral of the positive real ω to that of the positive imaginary frequency ξ, i.e., $\omega = i\xi$, and then the Casimir force can be written as

$$F_{\mathrm{C}} = \frac{\hbar}{2\pi^2}\int_0^\infty d\xi \int_0^\infty kdk\sqrt{\frac{\xi^2}{c^2}+k^2} \times \sum_{p=\mathrm{TE,TM}} \frac{r_p^{\mathrm{A}}(i\xi,k)r_p^{\mathrm{B}}(i\xi,k)e^{-2a\sqrt{\xi^2/c^2+k^2}}}{1-r_p^{\mathrm{A}}(i\xi,k)r_p^{\mathrm{B}}(i\xi,k)e^{-2a\sqrt{\xi^2/c^2+k^2}}}. \quad (2)$$

For numerical calculation, the variables ξ and k can be transformed into polar coordinates x and ϕ through $\xi/c \equiv \frac{x}{2a}\cos\phi$ and $k \equiv \frac{x}{2a}\sin\phi$; finally we find

$$F_{\mathrm{C}} = F_0\frac{15}{2\pi^4}\int_0^\infty x^3dx\int_0^{\pi/2}\sin\phi d\phi \times \sum_{p=\mathrm{TE,TM}} \frac{r_p^{\mathrm{A}}(x,\phi)r_p^{\mathrm{B}}(x,\phi)e^{-x}}{1-r_p^{\mathrm{A}}(x,\phi)r_p^{\mathrm{B}}(x,\phi)e^{-x}}, \quad (3)$$

where $F_0 = \hbar c\pi^2/240a^4$ is the well-known formula for the Casimir force between two perfectly conducting plates with separation a.

B. Effective medium theory for hyperbolic metamaterials (HMMs)

As the calculation of the Casimir force is very sensitive to the choice of effective medium model [20], we first introduce the micostructure of the HMMs and present the corrective effective medium theory suitable for it. As mentioned before, here we focus on the multilayer structure with alternating metal and dielectric layers, whose permittivities are given by ε_{m} and ε_{d}, respectively. Obviously, such structure is an anisotropic composite and must be described by the anisotropic Maxwell Garnett mixing formula [40]. To satisfy the homogeneity required by the effective medium theory, the thicknesses of the layers must be much smaller than the operating wavelength and the plasma wavelength; i.e., $d_{\mathrm{d}}, d_{\mathrm{m}} \ll \min\{\lambda_0, \lambda_p\}$. Then the effective permittivity tensor of the whole structure is given as [40]

$$\overleftrightarrow{\varepsilon} = \begin{pmatrix} \varepsilon_{xx} & 0 & 0 \\ 0 & \varepsilon_{yy} & 0 \\ 0 & 0 & \varepsilon_{zz} \end{pmatrix}, \quad (4)$$

with

$$\varepsilon_{xx} = \varepsilon_{yy} = f\varepsilon_{\mathrm{m}} + (1-f)\varepsilon_{\mathrm{d}}, \quad (5)$$

$$\varepsilon_{zz} = \left(\frac{f}{\varepsilon_{\mathrm{m}}} + \frac{1-f}{\varepsilon_{\mathrm{d}}}\right)^{-1}, \quad (6)$$

where f is the filling factor of the metal in the unit cell, and is defined by

$$f = d_{\mathrm{m}}/(d_{\mathrm{m}} + d_{\mathrm{d}}). \quad (7)$$

The z axis is chosen as the optical axis of the material. Due to these special effective permittivity tensors, the isofrequency dispersion relations display a unique feature when $\varepsilon_{xx}\varepsilon_{zz} < 0$, which is much different from the normal anisotropic metal or dielectric.

Since $\varepsilon_{xx} = \varepsilon_{yy}$, we only discuss the case of wave vectors being in the x-z plane. The dispersion relations can be achieved as [41]

$$k_x^2 + k_z^2 = \frac{\omega^2}{c^2}\varepsilon_{yy}, \quad (8)$$

for TE polarization, and

$$\frac{k_x^2}{\varepsilon_{zz}} + \frac{k_z^2}{\varepsilon_{xx}} = \frac{\omega^2}{c^2}, \quad (9)$$

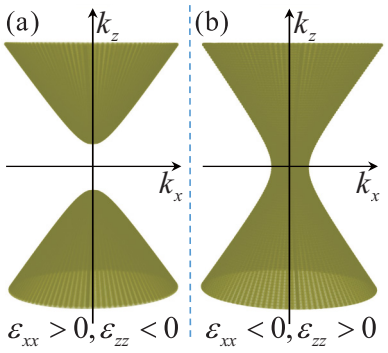

FIG. 2. Schematic illustration of the isofrequency contour in the wave-vector space of the HMMs for TM polarization with (a) type I: $\varepsilon_{xx} > 0$, $\varepsilon_{zz} < 0$ and (b) type II: $\varepsilon_{xx} < 0$, $\varepsilon_{zz} > 0$.

for TM polarization. Equation (8) describes a circle of k_x and k_z with radius $\omega\sqrt{\varepsilon_{yy}}/c$ when $\varepsilon_{yy} > 0$; this is the ordinary dispersion relation for dielectric. However, Eq. (9) describes an ellipse of k_x and k_z when both ε_{xx} and ε_{zz} are positive, but a hyperboloid of k_x and k_z when $\varepsilon_{xx}\varepsilon_{zz} < 0$. There are two kinds of hyperbolic contours for $\varepsilon_{xx}\varepsilon_{zz} < 0$. The first refers to $\varepsilon_{xx} > 0$ and $\varepsilon_{zz} < 0$; the hyperbolic contour is shown in Fig. 2(a), which is defined as type I HMM. The second refers to $\varepsilon_{xx} < 0$ and $\varepsilon_{zz} > 0$; the corresponding hyperbolic contour is shown in Fig. 2(b), which is defined as type II HMM. That is the reason why the uniaxially anisotropic materials with $\varepsilon_{xx}\varepsilon_{zz} < 0$ were named as hyperbolic metamaterials (HMMs).

According to Eq. (3), the reflection coefficients are key quantities to approach the Casimir force. Therefore we consider the reflective behavior of semi-infinite HMMs at first. The reflection coefficients incident from vacuum into HMMs can be derived and expressed as

$$\begin{aligned} r_{\mathrm{TE}} &= \frac{k_z^{\mathrm{i}} - k_z^{\mathrm{TE}}}{k_z^{\mathrm{i}} + k_z^{\mathrm{TE}}} \\ &= \frac{\sqrt{(\xi/c)^2 + k^2} - \sqrt{(\xi/c)^2\varepsilon_{yy} + k^2}}{\sqrt{(\xi/c)^2 + k^2} + \sqrt{(\xi/c)^2\varepsilon_{yy} + k^2}} \\ &= \frac{1 - \sqrt{\varepsilon_{xx}\cos^2\phi + \sin^2\phi}}{1 + \sqrt{\varepsilon_{xx}\cos^2\phi + \sin^2\phi}}, \end{aligned} \tag{10}$$

$$\begin{aligned} r_{\mathrm{TM}} &= \frac{\varepsilon_{xx}k_z^{\mathrm{i}} - k_z^{\mathrm{TM}}}{\varepsilon_{xx}k_z^{\mathrm{i}} + k_z^{\mathrm{TM}}} \\ &= \frac{\varepsilon_{xx}\sqrt{\left(\frac{\xi}{c}\right)^2 + k^2} - \sqrt{\varepsilon_{xx}\left(\frac{\xi}{c}\right)^2 + \frac{\varepsilon_{xx}}{\varepsilon_{zz}}k^2}}{\varepsilon_{xx}\sqrt{\left(\frac{\xi}{c}\right)^2 + k^2} + \sqrt{\varepsilon_{xx}\left(\frac{\xi}{c}\right)^2 + \frac{\varepsilon_{xx}}{\varepsilon_{zz}}k^2}} \\ &= \frac{\varepsilon_{xx} - \sqrt{\varepsilon_{xx}\cos^2\phi + \frac{\varepsilon_{xx}}{\varepsilon_{zz}}\sin^2\phi}}{\varepsilon_{xx} + \sqrt{\varepsilon_{xx}\cos^2\phi + \frac{\varepsilon_{xx}}{\varepsilon_{zz}}\sin^2\phi}}. \end{aligned} \tag{11}$$

The first lines of Eqs. (10) and (11) are written at the real frequency. Here k_z^{i} is the z component of the wave vector in vacuum and satisfies the relation $(k_z^{\mathrm{i}})^2 = K^2 - k^2$, where $K = \omega/c$. k_z^{TE} and k_z^{TM} are the z components of the wave vector in HMMs for TE and TM polarization, respectively. They are defined by Eqs. (8) and (9) as $(k_z^{\mathrm{TE}})^2 = K^2\varepsilon_{yy} - k^2$ and $(k_z^{\mathrm{TM}})^2/\varepsilon_{xx} = K^2 - k^2/\varepsilon_{zz}$. The second lines in Eqs. (10) and (11) have been obtained by converting the real frequency to the imaginary frequency, and we change the variables to polar coordinates in the third lines. It should be noticed that ε_{xx} plays a critical role in both TE and TM polarized reflection, but ε_{zz} only contributes to TM polarized reflection.

III. CASIMIR FORCE BETWEEN HYPERBOLIC METAMATERIALS

In this section, we begin to discuss the Casimir force between two HMMs. As the effective permittivity tensor of HMMs is determined by its ingredient metal and dielectric, we give the permittivity of metal and that of dielectric through the Drude model and Lorentz model, respectively, which are

$$\varepsilon_{\mathrm{m}} = 1 - \frac{\omega_{\mathrm{p,m}}^2}{\omega^2 + i\gamma_{\mathrm{m}}\omega}, \tag{12}$$

$$\varepsilon_{\mathrm{d}} = 1 - \frac{\omega_{\mathrm{p,d}}^2}{\omega^2 - \omega_{\mathrm{e,d}}^2 + i\gamma_{\mathrm{d}}\omega}, \tag{13}$$

where the $\omega_{\mathrm{p,m}}$ ($\omega_{\mathrm{p,d}}$) and γ_{m} (γ_{d}) are the plasma frequency and damping coefficient of metal (dielectric), respectively. $\omega_{\mathrm{e,d}}$ is the resonance frequency of the dielectric. Insert Eqs. (12) and (13) into Eqs. (10) and (11), and finally into Eq. (3), and the Casimir force can be evaluated. All frequencies are scaled with the reference frequency ω_0 and the separation a is measured in unit $\lambda_0 = 2\pi c/\omega_0$. If not stated otherwise, the characteristic frequencies of ingredient materials are chosen as follows: $\omega_{\mathrm{p,m}} = \omega_0$, $\gamma_{\mathrm{m}} = 0.006\omega_0$, $\omega_{\mathrm{p,d}} = 0.1\omega_0$, $\omega_{\mathrm{e,d}} = 0.25\omega_0$, and $\gamma_{\mathrm{d}} = 0.01\omega_0$.

A. Relationship with filling factor

In Fig. 3, the relative Casimir force $F_{\mathrm{r}} = F_{\mathrm{C}}/F_0$ between two identical HMMs for different filling factors f is numerically calculated. Because the two HMMs are identical and possess same electric and magnetic properties, the Casimir force between them are only attractive, i.e., $F_{\mathrm{r}} > 0$. The filling factor can change the effective permittivity tensor, i.e., in

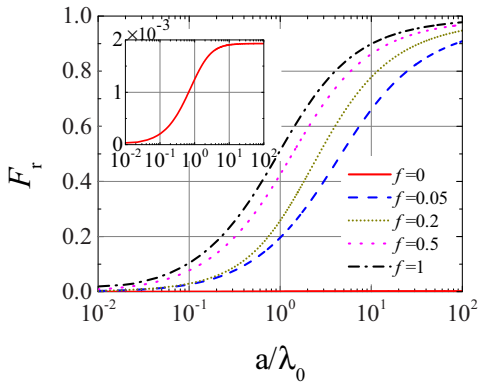

FIG. 3. The relative Casimir force between two identical HMMs for different filling factors as a function of separation. The inset shows the relative Casimir force for the case $f = 0$; i.e., the two media A and B are dielectrics.

Eqs. (5) and (6), and further affect the reflective coefficient and even the force. For example, in the case of $f = 0$, it refers to the Casimir force between two dielectrics with Eq. (13), and the relative force nearly disappears shown in the red solid curve in Fig. 3. When f increases, the relative force is enhanced monotonously for arbitrary separations. The common characters, shown in the curves of $f = 0.05$, 0.2, 0.5, and 1, are that (i) for minor separation, i.e., $a < 0.1\,\lambda_0$, $F_C \ll F_0$ so the relative force F_r is small and insensitive to filling factors; (ii) for moderate separation, i.e., $\lambda_0 < a < 100\lambda_0$, relative force is sensitive to filling factors; (iii) further, in case of large separation $a > 100\lambda_0$, relative force trends to 1 no matter the filling factor, which means $F_C \approx F_0 \to 0$. It should be noticed that the relative force F_r is the ratio of force F_C to the force between two perfectly conducting plates F_0 at the same separation. The increasing of relative force F_r with separation does not mean the increasing of force F_C with separation. The force F_C indeed decreases with separation in general. The case of $f = 1$ refers to the relative force between two metals with Eq. (12). The metal here is different from the perfectly conducting plate because a perfectly conducting plate is without dispersion and absorption [2].

The unique phenomenon observed here is that, comparing with the pure dielectrics, HMMs combined of metal and dielectric can dramatically strengthen the attractive Casimir force even if the filling factor of the metallic component is just 0.05, shown in the blue dashed curve in Fig. 3.

To extract the contribution of hyperbolic dispersion on the enhancement of the Casimir force, we present the real parts of the permittivity tensor $\varepsilon_{xx}(\omega)$ and $\varepsilon_{zz}(\omega)$ as a function of real frequency ω with two filling factors $f = 0.05$ and $f = 0.5$ in Fig. 4. As a comparison, we plot the corresponding reflectivity as function of imaginary frequency ξ and wave vector k in Fig. 5.

According to the definition of hyperbolic dispersion, it is clear that the mainly hyperbolic dispersion exists within the frequency band of $\omega < 0.2\omega_0$ for the case of $f = 0.05$, shown in Fig. 4(a). Correspondingly high reflectivity happens within the same frequency region spanning over all wave vectors k for the TM polarization, shown in Fig. 5(b). For the TE polarization, high reflectivity happens within the same frequency region but for the wave vector $k < 0.2k_0$. When the filling factor increases to $f = 0.5$, similar behavior happens but the mainly hyperbolic dispersion region extends to $\omega < \omega_0$. Therefore we can conclude that the hyperbolic dispersion leads

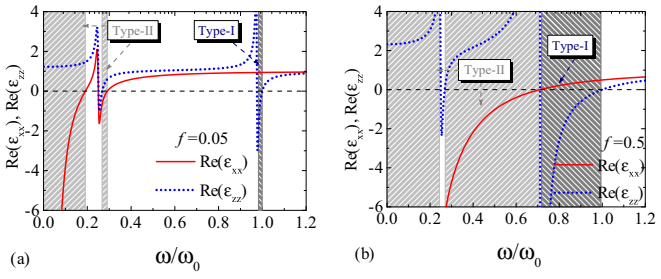

FIG. 4. The real parts of $\varepsilon_{xx}(\omega)$ and $\varepsilon_{zz}(\omega)$ as a function of ω with the filling factor (a) $f = 0.05$, (b) $f = 0.5$. Shadow areas indicate hyperbolic dispersion regions.

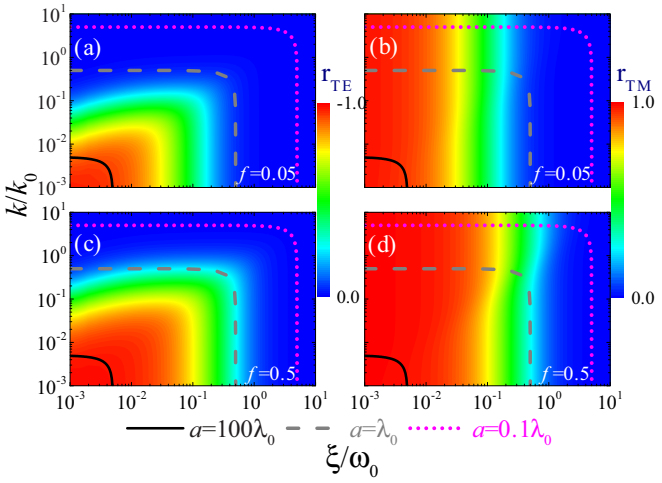

FIG. 5. (a) r_{TE} and (b) r_{TM} as functions of ξ and k with $f = 0.05$. (c) r_{TE} and (d) r_{TM} as functions of ξ and k with $f = 0.5$. Curves $2a\sqrt{\xi^2/c^2 + k^2} = 1$ for $a = 100\lambda_0, \lambda_0$, and $0.1\lambda_0$ are also plotted.

to high reflection in the imaginary frequency space. It is the unique feature of HMMs on the Casimir force.

From Eq. (2), the contribution of the electromagnetic model is embodied by the reflective coefficients. Besides, the term $\exp(-2a\sqrt{\xi^2/c^2 + k^2})$ in Eq. (2) acts as a truncated function; thus the electromagnetic modes inside the integral area S_{int}, which is surrounded by the curve $\sqrt{\xi^2/c^2 + k^2} = 1/2a$, are the main contributive modes to the Casimir force at separation a. We define the high reflective ratio N as $N = S_{\text{high ref}}/S_{\text{int}}$, where $S_{\text{high ref}}$ is the frequency-wave-vector region possessing high reflectivity ($|r_{\text{TE/TM}}|^2 > 0.9$) inside the integral area S_{int}. For perfectly conducting plates we know $|r_{\text{TE/TM}}|^2 = 1$ and from Eq. (3) we can easily get $F_r = 1$. Therefore N can reflect the amplitude of the force. We choose three separations ($a = 100\lambda_0$, λ_0, and $0.1\lambda_0$), and plot the boundary of S_{int}, i.e., $2a\sqrt{\xi^2/c^2 + k^2} = 1$ in Fig. 5. When $a = 100\lambda_0$, S_{int} surrounded by a solid curve is small, while $S_{\text{high ref}}$ is almost equal to S_{int} in all panels of Fig. 5; i.e., $N \approx 1$. As a result, the relative Casimir force moves to 1 clearly when $a > 100\lambda_0$. Similarly, when $a = 0.1\lambda_0$, S_{int} expands to dotted curves, and $N_{f=0.5} > N_{f=0.05}$; consequently the relative Casimir forces also satisfy $F_{r,f=0.5} > F_{r,f=0.05}$. If we further decrease the separation, S_{int} can be expanded further, but the ratio N should be smaller and trend to 0. Therefore, F_r would disappear when $a \ll 0.1\,\lambda_0$, as shown in Fig. 3. The force behavior shown in Fig. 3 can be easily understood according to the above analysis.

It should be noticed that the enhancement of the Casimir force on HMMs is the direct result of hyperbolic dispersion, not the ingredient metal. In the Appendix we calculate the relative Casimir force between two identical composite materials made of metallic particles dispersed in a dielectric matrix, whose components are also modeled by Eqs. (12) and (13). These complex media are described by the isotropic Maxwell Garnett mixing formula and treated as an isotropic medium. It shows that with the filling factor $f = 0.05$, the calculated Casimir force on these composite media is far weaker than that of Fig. 3. Therefore hyperbolic dispersion is essential to this huge enhancement of the Casimir force when fill factor f is small.

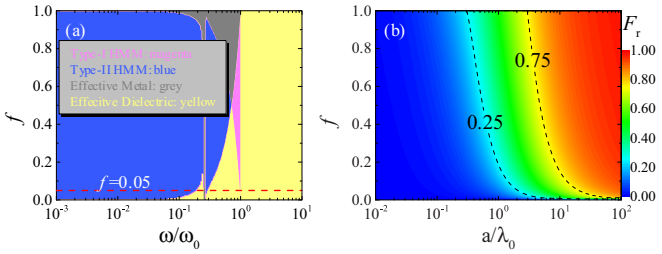

FIG. 6. (a) Optical phase diagram for the metal-dielectric multilayer system. (b) The relative Casimir force between two HMMs as a function of a and f. Parameters are the same as in Fig. 3.

In Fig. 6(a), we plot the optical phase diagram as a function of filling factor f. The regions of type I and type II HMMs are shown by the blue and magenta regions, respectively. Type II HMMs nearly occupy the lower frequency region of $\omega < 0.3\omega_0$. It is clear that the hyperbolic dispersion region increases monotonously with filling factor f when $f < 0.5$. Figure 6(b) shows the relative Casimir force as a function of f and separation a. It is easy to see that, by tuning the filling factor, the relative attractive force between two HMMs can be adjusted variably between the cases of metal or dielectric. Two dashed contour curves in Fig. 6(b) show the combination of f and a to get constant relative Casimir forces $F_r = 0.25$ and $F_r = 0.75$. For a certain value of the relative Casimir force, the thicker the metal, the less separation required. This means we can tune the attractive Casimir force by HMMs. When $f > 0.5$ in Fig. 6(a), though the proportion of hyperbolic dispersion region (in blue and magenta) is decreasing with f, the relative Casimir force is still increasing with f in Fig. 6(b). That is because the proportion of effective metal is also increasing, and the hyperbolic dispersion region combined with the effective metal region still increases and leads to a stronger Casimir force. For application, we can choose a suitable combination of f and a to get the Casimir force we want.

B. Relationship with characteristic frequencies

In the above section, we demonstrate that the relative Casimir force is related to the hyperbolic dispersion of HMMs because hyperbolic dispersion leads to high reflectivity similar to metal. Therefore the frequency band possessing hyperbolic dispersion determines the property of the Casimir force. Actually the frequency region possessing hyperbolic dispersion is not only determined by the filling factor but also by the character frequencies of its ingredient metal and dielectric.

These character frequencies are defined in Eqs. (12) and (13). We focus on the region of type II hyperbolic dispersion which is defined by Fig. 4, and calculate the bandwidth $\Delta\omega_{\rm HMM}$ possessing such hyperbolic dispersion as a function of various character frequencies in Fig. 7 under the constant $f = 0.05$. It indicates that the band becomes wider with increasing $\omega_{\rm p,m}$ or $\omega_{\rm p,d}$ when $\omega_{\rm p,d}$ or $\omega_{\rm p,m}$ is small, shown in Fig. 7(a). Figure 7(b) shows that the band becomes wider with increasing $\omega_{\rm p,m}$ and is not sensitive to $\omega_{\rm e,d}$. The band becomes wider with increasing $\omega_{\rm p,d}$ especially when $\omega_{\rm e,d}$ is around ω_0, as shown in Fig. 7(c).

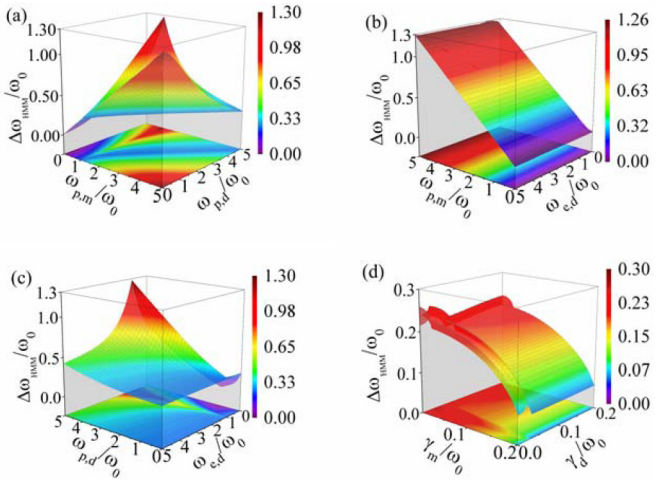

FIG. 7. The bandwidth $\Delta\omega_{\rm HMM}$ of type II hyperbolic dispersion as a function of the combination of two characteristic frequencies with filling factor $f = 0.05$. (a) $\omega_{\rm p,m}$ and $\omega_{\rm p,d}$,$\omega_{\rm e,d} = \omega_0$, $\gamma_{\rm m} = 0.006\omega_0$, and $\gamma_{\rm d} = 0.01\omega_0$; (b) $\omega_{\rm p,m}$ and $\omega_{\rm e,d}$,$\omega_{\rm p,d} = 0.1\omega_0$,$\gamma_{\rm m} = 0.006\omega_0$, and $\gamma_{\rm d} = 0.01\,\omega_0$; (c) $\omega_{\rm p,d}$ and $\omega_{\rm e,d}$,$\omega_{\rm p,m} = \omega_0$,$\gamma_{\rm m} = 0.006\,\omega_0$, and $\gamma_{\rm d} = 0.01\,\omega_0$; (d) $\gamma_{\rm m}$ and $\gamma_{\rm d}$, $\omega_{\rm p,m} = \omega_0$, $\omega_{\rm p,d} = 0.1\,\omega_0$, and $\omega_{\rm e,d} = 0.25\,\omega_0$.

Figure 7(d) shows that the stronger $\gamma_{\rm m}$ and $\gamma_{\rm d}$ result in the narrower width of the hyperbolic dispersion region.

We then study the relationship between the Casimir force and characteristic frequencies $\omega_{\rm p,m}$ or $\omega_{\rm p,d}$ following the fact that increasing $\omega_{\rm p,m}$ or $\omega_{\rm p,d}$ can expand the hyperbolic dispersion region. The dependence of the relative Casimir force on plasma frequency $\omega_{\rm p,m}$ and separation a is illustrated in Fig. 8(a), which shows that F_r monotonically increases with plasma frequencies for arbitrary a. It is obvious that ε_{xx} has been enhanced as plasma frequency $\omega_{\rm p,m}$ increases for lower imaginary frequencies; meanwhile ε_{zz} is about 1, as shown in Figs. 8(b) and 8(c). This means that increasing $\omega_{\rm p,m}$ leads to higher reflection in the lower imaginary frequency region. Therefore the Casimir force becomes stronger. Besides, as mentioned before, for large separation the Casimir force mainly comes from the contribution of lower frequencies. As a result, to achieve a certain value of relative force, the separation will become shorter with the increasing of plasma frequency $\omega_{\rm p,m}$, which can be seen at the dashed contours in Fig. 8(a). It should be noticed that the bandwidth of the hyperbolic

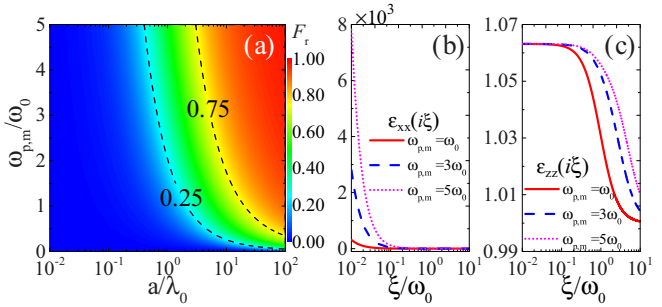

FIG. 8. (a) Contour plot of F_r as a function of a and the $\omega_{\rm p,m}$ with: $\omega_{\rm p,d} = 0.1\,\omega_0$,$\omega_{\rm e,d} = \omega_0$, $\gamma_{\rm m} = 0.006\,\omega_0$, and $\gamma_{\rm d} = 0.01\,\omega_0$. (b) ε_{xx} and (c) ε_{zz} as a function of ξ for different $\omega_{\rm p,m}$.

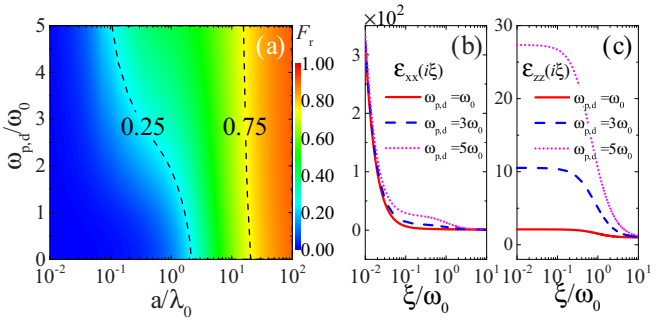

FIG. 9. (a) Contour plot of F_r as a function of a and $\omega_{p,d}$ with: $\omega_{p,m} = \omega_{e,d} = \omega_0$, $\gamma_m = 0.006\,\omega_0$, and $\gamma_d = 0.01\,\omega_0$. (b) ε_{xx} and (c) ε_{zz} as a function of ξ for different $\omega_{p,d}$.

dispersion increases with $\omega_{p,m}$, so expanding the hyperbolic dispersion bandwidth has the effect of strengthening the Casimir force.

Figure 9(a) illustrates the dependence of the force on $\omega_{p,d}$ and separation a. The behavior of the Casimir force fits the prediction in the above paragraph, i.e., the separation for a certain relative force becomes shorter with increasing $\omega_{p,d}$, shown by the 0.25 and 0.75 dashed contours in Fig. 9(a). It should be noticed that the 0.75 dashed contour looks almost like a vertical straight line. The reason is that for the corresponding separation $a \approx 20\lambda_0$, only the frequency region $\xi < 0.05\omega_0$ contributes to the Casimir force [11,20–22]. However, within such region, shown in Figs. 9(b) and 9(c), ε_{xx} is not sensitive to $\omega_{p,d}$ and ε_{zz} is tiny compared to ε_{xx}, so the Casimir force is also insensitive to $\omega_{p,d}$ when $a \approx 20\lambda_0$. Actually the slope of this line is still negative, which means the separation for $F_r = 0.75$ decreases slowly with increasing $\omega_{p,d}$.

IV. CONCLUSION

We have studied the Casimir effect between two HMMs which are made of alternative metal-dielectric layered structures. Based on the effective medium theory these structures could be treated as an anisotropic bulk media, and the effective permittivity tensors are extremely anisotropic and satisfy the relation $\varepsilon_{xx}\varepsilon_{zz} < 0$ in some frequency regions named the hyperbolic dispersion regions. As the force relates directly to the reflection coefficients of HMMs in mathematics, the reflection coefficients within hyperbolic dispersion regions are analyzed in detail. We demonstrate that the enhanced relative Casimir force is related to the hyperbolic dispersion because it leads to the high reflectivity similar to perfect conducting plates. Furthermore, the bandwidth of hyperbolic dispersion is dependent on the filling factor as well as the characteristic frequencies of ingredient materials. Therefore, the relations between the force and these parameters are discussed. We confirm that the magnitude of the force relates directly to the bandwidth of the hyperbolic dispersion. As the result, it is feasible to control the Casimir force by tuning the hyperbolic dispersion frequency region. This work could be helpful for HMMs to be used in microelectromechanical systems and nanoelectromechanical systems in the future.

ACKNOWLEDGMENTS

This work was partly supported by the National Natural Science Foundation of China (Grants No. 11274242, No. 11474221, No. 11574229, and No. 11504272), the Joint Fund of the National Natural Science Foundation of China (Grant No. U1330203), the 973 program (Grant No. 2013CB632701), Shanghai Science and Technology Committee (Grant No. 15XD1503700), and the Shanghai Education Commission Foundation the National Key Basic Research Special Foundation (Grant No. 2016YFA0302800).

APPENDIX: RELATIVE CASIMIR FORCE BETWEEN TWO IDENTICAL COMPLEX MEDIA DESCRIBED BY THE ISOTROPIC MAXWELL GARNETT MIXING FORMULA

Is hyperbolic dispersion essential to the huge enhancement of the Casimir force observed here?

To prove the essence of the hyperbolic dispersion, we choose an even simpler effective medium theory named "isotropic Maxwell Garnett mixing formula" to make a comparison. It is a simple but immensely successful theory which can describe the complex media as an isotropic medium. The isotropic Maxwell Garnett (IMG) mixing formula gives the isotropic effect permittivity ε_{MG} of the complex medium as [40]

$$\frac{\varepsilon_{MG} - \varepsilon_d}{\varepsilon_{MG} + 2\varepsilon_d} = f\frac{\varepsilon_m - \varepsilon_d}{\varepsilon_m + 2\varepsilon_d}. \tag{A1}$$

Here ε_d is the permittivity of the host dielectric while ε_m is the permittivity of the inclusion metal. The filling factor of the metal f should be much smaller than that of dielectric 1–f; then Eq. (A1) is applicable. Therefore, we describe our complex media by Eq. (A1) when f is small. In this situation, the relative Casimir forces are shown in Fig. 10 for different f.

Obviously the huge enhancement of the relative Casimir force disappears. Specifically, the relative forces in Fig. 3 are much stronger than those in Fig. 10, especially when the separation is large. Though in the case of $f = 0.5$ the relative force in Fig. 10 is enhanced, Eq. (A1) is inapplicable because the filling factors of two components are comparable. The Bruggeman theory is suitable for this situation and in

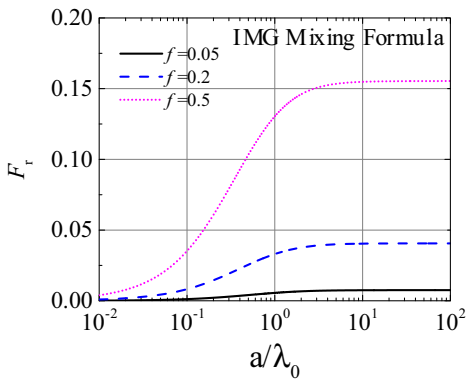

FIG. 10. The relative Casimir force between two identical complex media described by Eq. (A1) for different filling factors as a function of separation.

Ref. [20] the authors discussed the influence of different effective medium theories, including the Maxwell Garnett and the Bruggeman theories, on the Casimir force. The main conclusion is that the choice of effective medium approximation is critical in making precise comparisons between theory and experiment. Actually, Eq. (A1) is suitable for the complex medium which is spatially uniform and isotropic on average. For a layered structure, it is obviously anisotropic and must be described by the anisotropic Maxwell Garnett mixing formula, Eqs. (5) and (6). Consequencely, the hyperbolic dispersion is present and the results show the relative Casimir force is extremely enhanced. Therefore, the hyperbolic dispersion is essential to the huge enhancement of the Casimir force observed here.

[1] H. B. G. Casimir, Proc. K. Ned. Akad. Wet. **51**, 793 (1948).
[2] E. M. Lifshitz, Sov. Phys. JETP **2**, 73 (1956).
[3] M. Kardar and R. Golestanian, Rev. Mod. Phys. **71**, 1233 (1999).
[4] M. Bordag, U. Mohideen, and V. Mostepanenko, Phys. Rep. **353**, 1 (2001).
[5] M. S. Tomaš, Phys. Rev. A **66**, 052103 (2002).
[6] C. Raabe, L. Knöll, and D.-G. Welsch, Phys. Rev. A **68**, 033810 (2003).
[7] J. N. Munday, D. Iannuzzi, Y. Barash, and F. Capasso, Phys. Rev. A **71**, 042102 (2005).
[8] G. Bimonte and E. Santamato, Phys. Rev. A **76**, 013810 (2007).
[9] O. Kenneth and I. Klich, Phys. Rev. Lett. **97**, 160401 (2006).
[10] G. L. Klimchitskaya, U. Mohideen, and V. M. Mostepanenko, Rev. Mod. Phys. **81**, 1827 (2009).
[11] Y. Yang, R. Zeng, H. Chen, S. Zhu, and M. S. Zubairy, Phys. Rev. A **81**, 022114 (2010).
[12] C. Henkel and K. Joulain, Europhys. Lett. **72**, 929 (2005).
[13] V. Yannopapas and N. V. Vitanov, Phys. Rev. Lett. **103**, 120401 (2009).
[14] F. S. S. Rosa, D. A. R. Dalvit, and P. W. Milonni, Phys. Rev. Lett. **100**, 183602 (2008); Phys. Rev. A **78**, 032117 (2008).
[15] Y. Yang, R. Zeng, J. Xu, and S. Liu, Phys. Rev. A **77**, 015803 (2008).
[16] R. Zeng, Y. Yang, and S. Zhu, Phys. Rev. A **87**, 063823 (2013).
[17] R. Zeng and Y. Yang, Phys. Rev. A **83**, 012517 (2011).
[18] R. Esquivel-Sirvent, J. Appl. Phys. **102**, 034307 (2007).
[19] M. G. Silveirinha and S. I. Maslovski, Phys. Rev. A **82**, 052508 (2010).
[20] R. Esquivel-Sirvent and G. C. Schatz, Phys. Rev. A **83**, 042512 (2011).
[21] J. Sun, X. K. Hua, A. V. Goncharenko, and L. Gao, Phys. Rev. A **87**, 042509 (2013).
[22] J. Sun, Y. Huang, and L. Gao, Phys. Rev. A **89**, 012508 (2014).
[23] B. E. Sernelius, Phys. Rev. B **85**, 195427 (2012).
[24] A. G. Grushin and A. Cortijo, Phys. Rev. Lett. **106**, 020403 (2011).
[25] W. Nie, R. Zeng, Y. Lan, and S. Zhu, Phys. Rev. B **88**, 085421 (2013).
[26] R. Zeng, L. Chen, W. Nie, M. Bi, Y. Yang, and S. Zhu, Phys. Lett. A **380**, 2861 (2016).
[27] A. Poddubny, I. Iorsh, P. Belov, and Y. Kivshar, Nat. Photonics **7**, 948 (2013).
[28] P. Shekhar, J. Atkinson, and Z. Jacob, Nano Convergence **1**, 1 (2014).
[29] C. L. Cortes, W. Newman, S. Molesky, and Z. Jacob, J. Opt. **14**, 063001 (2012).
[30] A. J. Hoffman, L. Alekseyev, S. S. Howard, K. J. Franz, D. Wasserman, V. A. Podolskiy, E. E. Narimanov, D. L. Sivco, and C. Gmachl, Nat. Mater. **6**, 946 (2007).
[31] Z. Jacob, I. I. Smolyaninov, and E. E. Narimanov, Appl. Phys. Lett. **100**, 181105 (2012).
[32] H. N. S. Krishnamoorthy, Z. Jacob, E. Narimanov, I. Kretzschmar, and V. M. Menon, Science **336**, 205 (2012).
[33] A. N. Poddubny, P. A. Belov, and Y. S. Kivshar, Phys. Rev. A **84**, 023807 (2011).
[34] S.-A. Biehs, M. Tschikin, and P. Ben-Abdallah, Phys. Rev. Lett. **109**, 104301 (2012).
[35] S.-A. Biehs, S. Lang, A. Y. Petrov, M. Eich, and P. Ben-Abdallah, Phys. Rev. Lett. **115**, 174301 (2015).
[36] Z. Jacob, L. V. Alekseyev, and E. Narimanov, Opt. Express **14**, 8247 (2006).
[37] Z. Liu, H. Lee, Y. Xiong, C. Sun, and X. Zhang, Science **315**, 1686 (2007).
[38] J. Yao, Z. Liu, Y. Liu, Y. Wang, C. Sun, G. Bartal, A. M. Stacy, and X. Zhang, Science **321**, 930 (2008).
[39] M. A. Noginov, Y. A. Barnakov, G. Zhu, T. Tumkur, H. Li, and E. E. Narimanov, Appl. Phys. Lett. **94**, 151105 (2009).
[40] V. A. Markel, J. Opt. Soc. Am. A **33**, 1244 (2016).
[41] L. Hu and S. T. Chui, Phys. Rev. B **66**, 085108 (2002).